Engineering Geological Assessment of Lin Ma Hang Mine Caverns Using Handheld LiDAR Scanner

Samson Leung*, Geoffrey Pook, Ming Kwok, Cloud Lo, Michael Wright

Meinhardt Infrastructure and Environment Ltd., Hong Kong, China

*Corresponding author
doi: https://doi.org/10.21467/proceedings.133.10

ABSTRACT

Lin Ma Hang Mine, in the former closed border zone in the northeast New Territories, rewards intrepid visitors with impressive 19th century mine caverns. As part of the planned establishment of the Robin's Nest Country Park, the caverns have been earmarked for revitalization to increase public awareness and accessibility. A key aspect of the scheme is to assess the stability of the accessible caverns. Maintaining the natural heritage and appearance of the historical mine workings is forefront in tailoring specific solutions. Faced with a highly irregular cavern layout due to a complex history of mining activities, the engineering geological assessment was facilitated by 3D digitalisation of the cavern developed from handheld and aerial LiDAR scanning. Point cloud data obtained provided a fast and efficient means to form models for 3D and 2D assessment and visualisation. The ability to handle data through GIS and Common Data Environments (CDE) means management of vast point cloud sets is no longer a daunting task. The digital model developed will be showcased as part of the planned public engagement and educational information about the capabilities of digital geoscience and also to further explore in virtual reality the mine cavern extent.

Keywords: LiDAR, Automated Rock Joint Recognition, Abandoned Mine Survey

1 Introduction

1.1 Site description

The Government of the Hong Kong Special Administrative Region (HKSAR) plans to revitalize the Lin Ma Hang Lead Mine site as a Country Park Outdoor Education Site showcasing the heritage mining history and ecology of the area to the general public. This includes the revitalization of an existing mine cavern, natural terrain hazard mitigation and other necessary works such as to promote access to the cavern for visitors. The Lin Ma Hang Lead Mine is an abandoned mine site operated intermittently from the 1860s until 1962. It is a significant historical mining site with a rich heritage linked to the local villages and military conflict legacy that contains one of Hong Kong's most complex mining operations in a remote wilderness area. Located in the Sha Tau Kok area of Hong Kong east of Heung Yuen Wai and north of Robin's Nest, the lower slopes of the mine about the Lin Ma Hang Road and Sha Tau Kok Closed Frontier Road at the border between Hong Kong and Shenzhen (SEZ). The Lin Ma Hang Lead Mines SSSI is related to the caverns and contains one of the most important bat colonies in Hong Kong (Figure 1).

The mineralisation that gives the mine its significant resource results from metamorphism of the coarse ash tuff with a series of en-echelon, northwest-southeast striking, north-easterly dipping vein deposits. The ore veins generally dip between 15° and 60°, with some veins nearly vertical. The veins are lenticular along strike and down dip, with widths of a few millimetres to several metres and a strike length of some 2km.

Proceedings DOI: 10.21467/proceedings.133; Series: AIJR Proceedings; ISSN: 2582-3922; ISBN: 978-81-957605-1-0

Figure 1: Lin Ma Hang Mine Location

General view of the mining compound in 1938; looking from the Chinese border (Williams 1991).

Plate 1: Lin Ma Hang Mine Mill Processing Buildings 1938, Williams 1991

The mine was developed by a series of adits at different levels and locations. Since the mine has been worked and reworked by different parties at different times during the past, there are varying accounts about the extent and locations of the mine workings. The mine level number referencing system has also changed over the years but at least five major levels are recorded: Levels 1, 2, 3, 5 and 6. Level 1 access is on the Lin Ma Hang "Border Road", with other levels at progressively higher elevations. The caverns which are the subject of this study are mainly on the uppermost level – Level 6.

A substantial development of mill buildings and ore processing plant with tailings dump area was constructed to the northeast of the mining area (Plate 1). Several transport adits were driven from the underground workings towards the mine-processing plant buildings. During WWII, the Japanese mined most of the ore in the eastern section of the mine by robbing pillars, resulting in some caving of the roof. They also drove an additional intermediate level between the pre-War uppermost Levels 5 and 6. The mine eventually shut down during the period 1958-1962. Since then, the Lin Ma Hang Mine has been abandoned without operations or any maintenance. Up to 2016, the mine was within the Frontier Closed Area (FCA) and so out of bounds for most members of the public. In 2019, steel grilles were installed at selected adit entrances of Level 3 and Level 6 to prevent public entry and disturbance of the bat colonies. No abandonment mine plans have been located and the contemporary documentation of the mine workings is fragmentary. Davis et al (1956 and 1964) includes a plan based on a somewhat schematic and generalized map prepared by S.K. Wong in 1953 showing Level 5 and Level 6 and several presumed surface buildings in the Caverns area (Figure 2). Williams et al (1991) consolidated the available information supported by inspection and survey within Level 2 and 3 by the Geotechnical Control Office (GCO now GEO). A detailed recent account of the mine history is provided in Mellor, T. (2018a, 2018b, 2018c, 2021).

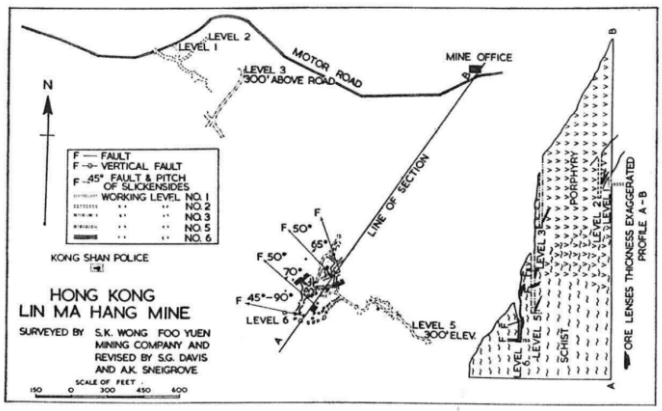

FIG. 2. Map of Lin Ma Hang Lead Mine with profile of the four main levels of exploitation.

Figure 2: Lin Ma Hang Mine Plan, Davis et al 1964

Proceedings DOI: 10.21467/proceedings.133
ISBN: 978-81-957605-1-0

Series: AIJR Proceedings
ISSN: 2582-3922

2 Objectives

2.1 Geotechnical Assessment

The geotechnical study aims to assess the existing layout, condition and stability of the accessible cavern at Level 6 and adjacent related adits and shafts such that any necessary stabilization works can be designed to reduce the risk to public visitors whilst at the same time preserving the existing industrial heritage and ecology of the area. The study is based on the following steps: (i) understanding the existing cavern network; (ii) evaluating the rock mass condition within the cavern; and (iii) conducting analytical and numerical analysis.

2.2 Understanding the existing cavern network

The generalized mine plan prepared by S.K. Wong in 1953 suggests the Level 6 cavern was an E-W trending opening/ mine stope surrounded by several sub-rounded shaped rock pillars. Subsequent mine mapping by handheld laser scanner reveals the Level 6 cavern is part of an inter-connected room-and pillar- mine workings with several branches of adits trending S-N and E-W, as well as several production shafts connected to the ground surface and the lower mine levels. Mine mapping provides fundamental information for geotechnical assessment namely the numbers of rock pillars supporting the cavern, dimension of the rock pillars, and the spatial relationship between the cavern and the pillars. Preliminary geotechnical assessment was conducted by calculating pillar width-height ratio and estimating applied pillar stress due to overburden. Empirical stability graph method was applied to assess the pillar stability with respect to the minimum FOS required in Hong Kong.

2.3 Evaluation of rock mass condition

Engineering rock mapping was carried out in the cavern and adits to evaluate the rock mass condition as well as recording rock discontinuities data. Rock mass classification systems namely Q-System, RMR, and GSI were used to evaluate the general rock mass quality. Rock stability kinematic analysis by conventional stereographic projection was conducted based on the discontinuities data extracted by handheld laser scanner. Potential failure mechanism namely planar failure on the sidewall and gravity-driven wedge fallout from the crown was examined as part of the geotechnical assessment. The bedrock of the caverns area is characterised by dark grey to brownish grey, moderately weathered, strong to moderately strong, Grade II/III coarse ash Tuff. A relatively thin soil layer comprising colluvium overlies rock head with limited in-situ weathering profile developed above the Caverns. The entrance into the main cavern gallery and several adit entrances are excavated into the face of a steep, locally overhanging rock cut slope (Plate 2). The rock cut slope (Feature no. 3NE-A/C79) up to 10.5m high surrounds a bowl-shaped excavation, “the atrium”.

Plate 2: The rock slope and entrances into the main Level 6 cavern

2.4 Analytical and Numerical Analysis

Subsequent analysis will be based on the results of field surveys and planned GI. Limit equilibrium method will be used to calculate FOS against different potential failure mechanisms. Loading condition will be based on mapped block size and overburden pressure with rock strength parameters derived from in-situ tests and field measurement. Numerical analyses by computer software Phase^2 will be carried out for critical cavern sections. Generalized Hoek-Brown failure criterion will be used to evaluate the rock mass with a range of GSI values.

2.5 Potential Stabilisation Measures

Typical measures, including rock dowels, wire mesh and buttresses, will be considered as enhancement of the local stability of the caverns. The key approach for exploring necessary stability measures in Lin Ma Hang Cavern aims to maintain wherever practical the natural and mining heritage of the site and to preserve the authentic appearance and impression of the caverns. The scheme aims to protect the natural ecological niche currently notably occupied by several species of bats whilst also utilizing the rock strength and cavern layout to reduce the requirements for any conventional systematic support, as well as providing safe walkways for public access. The enhancement works will include sympathetic finishes and styles to ensure that the natural heritage and appearance of the caverns can be preserved.

3 Methodology

3.1 Data Collection

The site is remote and largely covered with dense vegetation and tree cover. To build up the site history and existing topography, information from various sources was gathered and collated. Due to the site constraints and large site area a traditional site-specific topographical survey was impractical within the desk study time frame. The existing data gathering processes are listed in Table 1.

Table 1: Existing data gathering process

Data		Sources	Description
1	Open Data		
1.1	Topographical Maps iB1000	Retrieved from Lands D Map Service 2.0	Traditional base maps in CAD format with contours presented every 2m interval
1.2	2010 LiDAR Dataset	Requested from GEO	Hong Kong territory-wide Light Detection and Ranging Survey in 2010 with 0.50m Point Density
1.3	2020 LiDAR Dataset	Requested from GEO	Hong Kong territory-wide LiDAR in 2020 with 0.25m Point Density
2	Desk Study Data		
2.1	Aerial Photographs (AP) from 1924	Borrowed from GEO AP Library	Aerial survey undertaken by the Government or the British Royal Air Force (RAF) in a yearly bases.
2.2	Old maps or old mine plans	Various sources, most importantly from Williams (1991)	Summary of the Lin Ma Hang Lead Mine from GEO revisit including the history and the conditions back in year 1991. (Williams, 1991)
3	Project Specific Data		
3.1	Traditional site walkover survey	Meinhardt Team	Major site walkover survey tasks include but not limited to: ▪ Making notes on LiDAR generated contoured topographic maps, record with sketches and descriptions of significant observations

Proceedings DOI: 10.21467/proceedings.133
ISBN: 978-81-957605-1-0

Series: AIJR Proceedings
ISSN: 2582-3922

Data		Sources	Description
			▪ Measuring dimensions with measuring tape, laser detector, directions and orientation with geological compasses. ▪ Recording the absolute location with GPS or relative location with reference to the pre-existing topographical plan
3.2	UAV (Drone) Data	Meinhardt Team	Drones are applied to take vertical, oblique aerial HD video and still photographs to discover significant detectable features on the ground surface and understanding the area and its context
3.3	Traditional topographical survey	Surveyor Team	Major topographical survey tasks include: ▪ Production of topographical contours of 1m interval, which may include computer smoothing and modification ▪ Outline significant structures, utilities and trees. And in the special case of cavern, the top and bottom of the cavern entrance and cave in, if any
3.4	Point Cloud Data	Meinhardt Team	GeoSLAM handheld scanner is applied to collect Point Cloud data with range up to 100m with in-built video camera and using georeference spheres. Two sets of data are collected during the scanning: ▪ Points with relative geometry with reference to the initial starting location (Local XYZ) & ▪ Video of throughout the scanning to record visual data (RGB / actual conditions seen in the study area) The cavern area and adits are scanned in separate parts due to topographical difference, accessibility & safety issues, namely: ▪ Atrium area of different elevation ▪ Rock Slopes ▪ Main cavern gallery ▪ Adits & other massive cavern areas behind grilles ▪ Adits & cavern areas at other mine levels ▪ Shafts/ surface collapses

3.2 Data Processing

Following gathering of data from the sources outlined in Table 1, data processing and analysis are undertaken to generate ground models and extract geotechnical design parameters (Table 2).

Table 2: Data processing

Steps		Software	Description
1	Forming Overall Point Cloud Cavern Model		
1.1	Initial Processing	GeoSlam Hub & CloudCompare Stereo v. 2.12	▪ Retrieve all point cloud data parts, check and choose the best possible scan in multiple scan trials. ▪ Convert point cloud from. geoslam format to .laz format via GeoSlam Hub ▪ Subsample the point cloud in order to process further in a reasonable speed
1.2	Georeferencing	CloudCompare Stereo v. 2.12	Since the point cloud data are collected in a series of scan portions, there are two major parts in Georeferencing, namely

Steps		Software	Description
			▪ Absolute Georeferencing - the major scan of the Cavern area is put to its absolute spatial location based on the Georeference spheres and their GPS readings ▪ Point Cloud merging (Relative Georeferencing) - other point cloud scan parts are merged onto the major scan with absolute spatial location by recognition of distinct site geometry and reference points at the Cavern area. ▪ Additional Checking - afterwards, the exposed surface part of the point cloud model is checked against the LiDAR Data to match the overall surface topography layout
1.3	Noise cleaning	CloudCompare Stereo v. 2.12	A series of noise cleaning methods are adopted in the Cavern Model: ▪ Typical built-in noise cleaning in CloudCompare to remove statistical outliers, including the SOR Filter and Noise Filter Scan time clipping - noise/ inaccurate point data in particular scan time are removed. The inaccuracy is usually associated with data collection errors where relative spatial references cannot be recognized by the scanner at particular time intervals. In the case of this cavern study, the error usually occurs when (1) traversing in and out of confined areas, (2) scanning involves trees and/or moving objects in the surroundings ▪ Elevation clipping- noise/ inaccurate point data on particular range and values of elevation are removed. This is particularly useful with reference with the LiDAR data to remove vegetation cover at the atrium ▪ Manual clipping - in the end, the point cloud model is checked, any noise/inaccurate point data left are removed with reference to actual field observations by professional judgement
2	Using Overall Point Cloud Cavern Model		
2.1	Extracting the Cavern geometry	CloudCompare Stereo v. 2.12 & CAD Softwares (Microstation and AutoCAD)	After the overall point cloud model is built, 2D views such as cavern sections (cutting along the X or Y axis) and layouts (cutting along the Z axis) can be formed freely by slicing and sampling a certain thickness of the point cloud via "Cross Section" and extracting contours. Whereas elevations can also be extracted, but require unfolding of the point cloud along an elevation section line. The extracted sections, layouts and elevations are in CAD (.dxf) format for further edits or use.
2.2	3D Cavern Model	CloudCompare Stereo v. 2.12 & Leapfrog Works	Overall point cloud model can be meshed using functions and plugins in CloudCompare – "Delaunay for 2.5D Clouds" and "Poisson Surface Reconstruction for 3D Clouds". Afterwards, the mesh can be extracted and imported in Leapfrog Works for better visualization with a 3D topographical model.
2.3	Rock Joint Analysis	CloudCompare Stereo v. 2.12 & Dips v6.0	Different portions of the point cloud model, such as rock slope faces, can be isolated. The portion can then be classified into planes via plug-in "Facet/fraction detection" in CloudCompare. The orientation and dip direction of the planes can then be transformed and analysed in Dips v6.0, to identify any potential kinematic hazards
2.4	Cavern Stress Analysis	CloudCompare Stereo v. 2.12 & Phase^2 v9.0	Critical profiles of the cavern are extracted into CAD files and the profiles are imported and analysed with Phase^2 to simulate 2D Stress conditions of the cavern and identify potential areas of concern.

Proceedings DOI: 10.21467/proceedings.133
ISBN: 978-81-957605-1-0

Series: AIJR Proceedings
ISSN: 2582-3922

4 Analysis & Discussion

The point cloud data obtained from the cavern and mine area was used in various ways to provide engineering geological assessment. The value of this data is in the ease of the collection, as well as the quality and quantity of data obtained. As the aim of the works was to verify the stability and provide necessary enhancement schemes, it was critical that the point cloud provided both a highly accurate and fully interactive representation of the accessible mine. The following areas are discussed with reference to how the 3D scanning process produced high quality output in an atypical working environment.

4.1 Geospatial

The existing documentation on the extent and layout of the mine is very limited; however, it is important to understand the original context of the mining to be able to re-create the network. The mines were excavated over a series of stages by different operators for various purposes and using different mining techniques. This has left a rather haphazard arrangement of openings, shafts, adits, pillars and rooms. By scanning and reproducing the 3D mesh in relation to the latest high resolution 2020 aerial

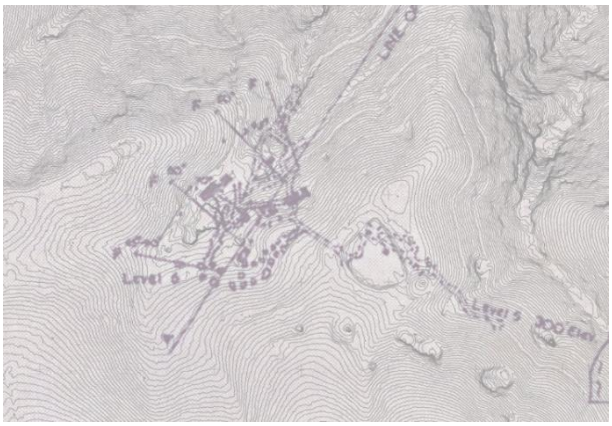

Figure 3: Lin Ma Hang Mine Level 5 & 6 plan from Davis et al 1964 and contoured 2020 aerial LiDAR

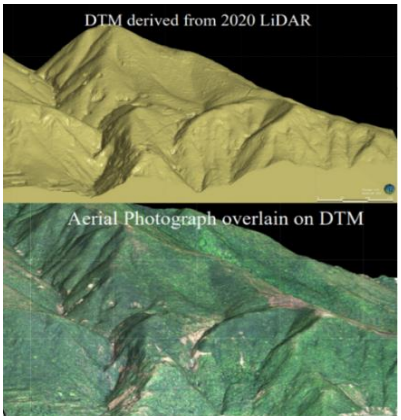

Figure 4: Lin Ma Hang Mine 2020 aerial LiDAR DTM and photo drape

LiDAR data (Wong, 2021), the extent of the excavation in relation to the surface features, rock and soil overburden, clearance between mine levels, potential shaft and adit connections is revealed, as well as relating findings to desk stuzdy data obtained through old mine maps and layout drawings (Figure 3). Hillshade and aerial photos draped over LiDAR generated DTM were created (Figure 4).

As with a traditional survey, the surfaces can be mapped but in this case the task involves a 3D excavation with pillars and arched crowns up to 6m high (Figure 5). The irregular shape, thickness and orientation can be accurately modelled in georeferenced space with respect to the surface topography

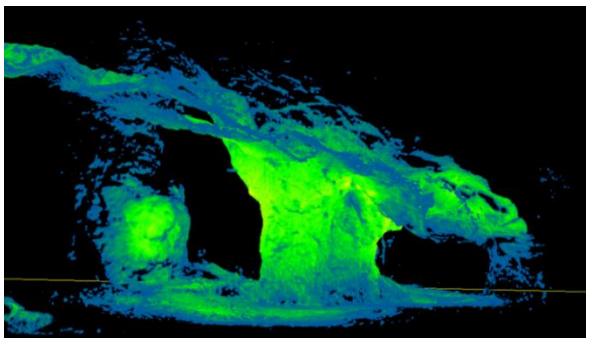

Figure 5: Lin Ma Hang Mine 3D scanning point cloud heat map

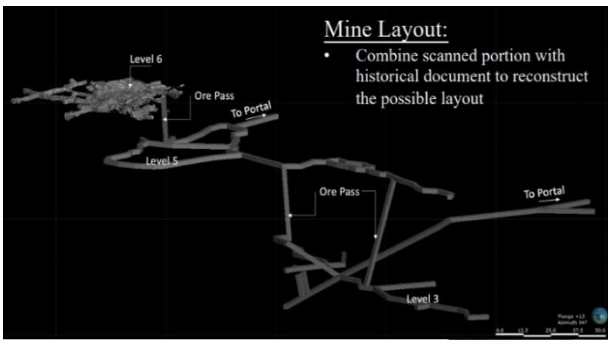

Figure 6: Lin Ma Hang Mine 3D layout with the Level 6 caverns area at top left. The model for Level 5 and Level 3 are based on interpretation of plans in Davies et all 1964 and Williams 1991

and control points. It is noted that slight offset of data may arise during the point cloud merging during relative georeferencing. In order to enhance the accuracy, each point cloud scan was to contain at least one locally fixed feature, such as the Grilles, for matching purposes. By developing a 3D ground model in GIS/ LeapFrog software, the scan data is easily matched to the surface expressions. The extent of the Level 6 sub layer could be determined as well as the proximity of unconnected adits beneath the hiking trail. It is important to correlate the surface expressions with the subsurface features and, by utilizing the 2020 LiDAR, drone surveys and site reconnaissance, it was possible to develop a better) understanding of the mine layout above and below ground (Figure 6).

The cavern is entered through three rock arches separated by four substantial rock pillars at the southern edge of the atrium (Plate 3). The ground level of the cavern gallery varies between +180 to +185 mPD, similar to that of the atrium level. The inner southern part of the gallery is marked by entrances to several adits separated by rock pillars or ribs. Adits are fenced off by lockable metal grilles installed in 2019, where the grille openings are large enough to allow passage of bats and uninterrupted natural ventilation (Plate 4). One adit terminates at a vertical unlined shaft, which is open at the ground surface next to the footpath access to the caverns.

Plate 3: The Level 6 cavern

The lateral span of the gallery has a maximum dimension of 19m. The maximum crown height in the gallery is around 6m near the entrance archway. The typical crown height is around 4m, descending to 3m against the eastern wall, Site surveys identifies several rounded to square shaped rock pillars and some elongated rib pillars around the cavern gallery. Pillars forming the entrance archways are formed in jointed volcanic Tuff rock. They exhibit occasional slickensided surfaces and open joints. Existing rock rubble packing are found around the bases of some pillars. A total of 10 major adits, some of which are interconnected have been identified (Figure 7).

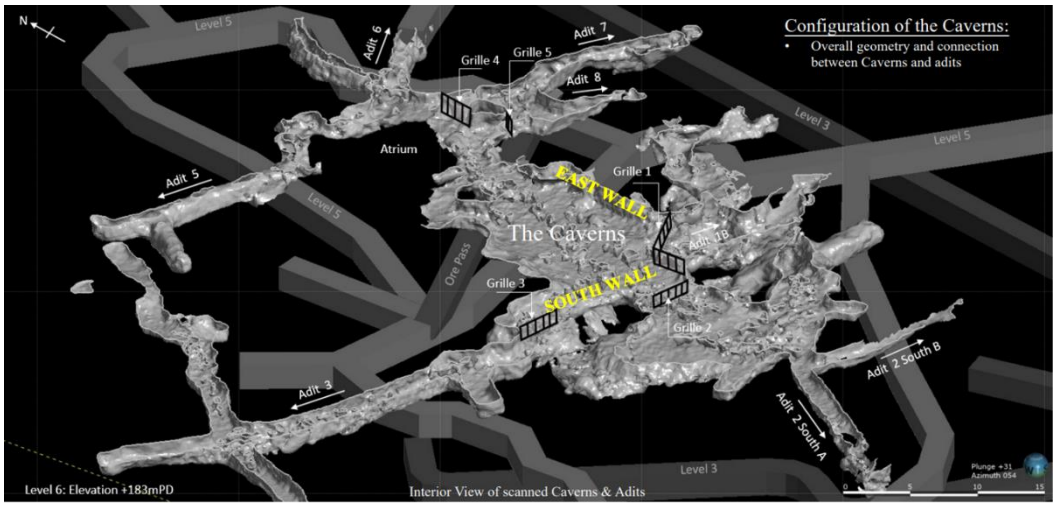

Figure 7: Lin Ma Hang Mine Level 6 cavern and adits 3D meshed model

Proceedings DOI: 10.21467/proceedings.133
ISBN: 978-81-957605-1-0

Series: AIJR Proceedings
ISSN: 2582-3922

The adits observed are mostly sub-horizontal at around +180mPD. These adits are part of the previously described Level 6. A lower level at +174 mPD approx. was also identified. This is suspected to be the intermediate level between Level 5 and Level 6. The major adits fork or branch into multiple galleries, forming an inter-connected room and pillar mine network. Site inspection identifies mortar cemented rock rubble walls are built between some pillars, blocking the connection between adits. All accessible adits are excavated in rock and are unlined. The remnants of disused vertical timber prop supports are present in the adits. Site inspections also confirmed a lower level (Level 5) mine network, accessible via two adit entrances at approximately +157mPD, northeast of the caverns. A total of 4 shafts connected to Level 6 have been located. The shafts are formed in rock, square or rectangular in plan and unlined. One of the shafts connects to the surface while three are suspected to connect to lower-level workings (Plate 4).

Plate 4: A shaft in Level 6 connecting to lower-level workings

The results of scanning and site inspection reveal the cavern gallery entrance of rock arches within the rock cut slope. These details were captured in 3D for use in the model from the point cloud scanning. The southern extent of the Level 6 cave is bounded by a persistent sub-vertical plane trending WNW-ESE which forms the northern faces of some pillars and the southern wall of an adit. The plane represented in the 3D model can be tentatively correlated with fault/shear zones, indicated on the 1950s mine plan, Davis et al (1964) (Figures 2 and 3).

4.2 Geotechnical

The point cloud model created from the 3D scanning was incorporated in the assessment of the design sections and elevations as well as for using in the empirical assessment of rock mass classification Q-system and as direct input in 2D FEM. As the project scope required an assessment of the overall stability of the existing caverns, the point cloud model is particularly useful in providing actual cavern geometry, such as Cavern spans and areas of high and low cover, and joint measurements. Critical spans and areas of stability concerns are identified and sections can be readily extracted for further review, analysis and markup. These methods allowed a comprehensive review of the stability of the opening in terms of stress and spans. Without a comprehensive 3D model detailing the extent and arrangement of pillars, openings and adits, the identification of critical spans and areas of high or low cover would have been challenging to determine.

Based on site inspection and details obtained from the scan, Q-value and RMR parameters were determined for the cavern areas (Table 3 and Table 4). RMR rating is calculated as 58.

Table 3: Q-values for the caverns

	Cavern Portion (Refer to Figure 10 for the Location)		
Parameter	Wall (East)	Wall (South)	Roof (crown)
RQD	75	75	80
Jn	9	12	9
Jr	1.5	0.5	1.5
Ja	2	4	2
Jw	0.66	1	1
SRF	2.5	2.5	2.5
Calculated Q	1.65	0.32	2.67

Table 4: RMR parameters for the caverns

Parameter	Value	Rating
UCS	Estimated 50 MPa	7
RQD	50 – 75%	13
Joint Spacing	0.6 – 2m	15
Joint Condition - Persistence	Most joints are 3 – 10m long	2
Joint Condition – Separation	Most joints have 1 – 5mm aperture	1
Joint Condition – Roughness	Most joints have slightly rough to smooth surface	1
Joint Condition – Infilling	Most joints are clean	6
Joint Condition – Weathering	Most joints are moderately weathered with stained surface	3
Groundwater	Damp	10

GSI values ranging from 50 to 60 were considered in our simulation to reflects the nature of moderately weathered with interlocked undisturbed blocky rock mass occurs in the cavern.

A series of rubble walls or surface protection were identified during site inspection as part of the original mine workings. The exact purpose of these features is lost to time but they appear to backfill undercut pillars or to provide rubble walls between pillars. It is not clear if these are designed as storage of the mine tailings or to provide a stabilizing function. The extent, thickness and shape, was better understood and illustrated with the benefit of scanning and viewing in 3D.

4.3 Kinematic Analysis

A feature of the point cloud data is the ability to carry out statistical analysis of the points to derive facets, or surfaces, which can be correlated to rock joints of the exposed mine faces. As the mine is already fully excavated, the scanning data was ideal for obtaining the joints in a fully 3D space. This allowed an accurate representation of joints in rock faces and within the pillars and also those that interface with both walls and crown of the adits and cavern. This is an invaluable tool to assist the traditional rock joint mapping (Figure 8).

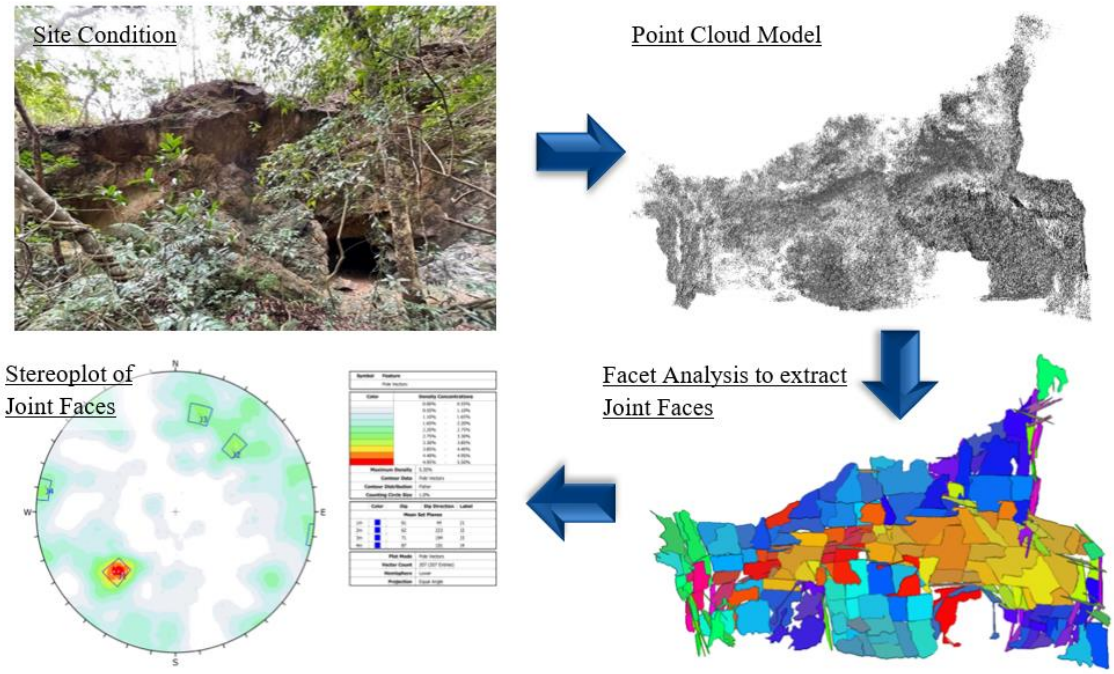

Figure 8: Lin Ma Hang Mine (Northeast side of the Atrium). Facets and stereoplot generated from 3D scanning point cloud

Proceedings DOI: 10.21467/proceedings.133
ISBN: 978-81-957605-1-0

Series: AIJR Proceedings
ISSN: 2582-3922

Portable laser scan and conventional manual discontinuity survey were carried out for the rock faces (Table 5 and Table 6). Facets extracted from 3D point cloud laser scanning and manual mapped discontinuities consisting of rock joints with occasional shear planes and quartz veins are plotted into stereonets. Separate stereonet plots representing manual survey data and laser scan data are produced for northeast, southeast, and northwest slope faces. Pillars near the archway entrance exhibit adverse joint orientations that can be mapped through the pillar shape by facet identification (Figure 9), while one pillar is characterised by longitudinal cracks (i.e. crack formed by spalling along the long axis of the pillar) and associated fractured rock materials. Irregular cracks and open joints are not as clear to identify in the scanning data and require visual inspection. Other pillars in the cavern gallery show no sign of adverse jointing or intense cracking and fracturing. Due to the quantity of the data, the major joints sets are predominantly determined through the scanning data with traditional mapping providing an additional assessment through contextual site observation.

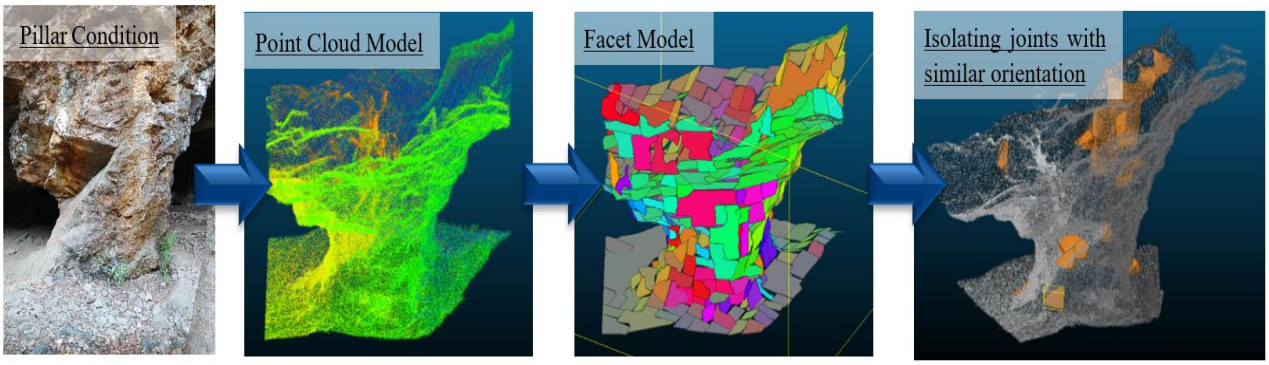

Figure 9: Process of facet identification through a pillar

Table 5: Major joint set data from discontinuity survey for the overall Cavern Area

Major Joint Set	Manual Discontinuity Survey	
	Dip Angle	Dip Direction
J1	43	117
J2	76	023
J3	42	044
J4	79	183

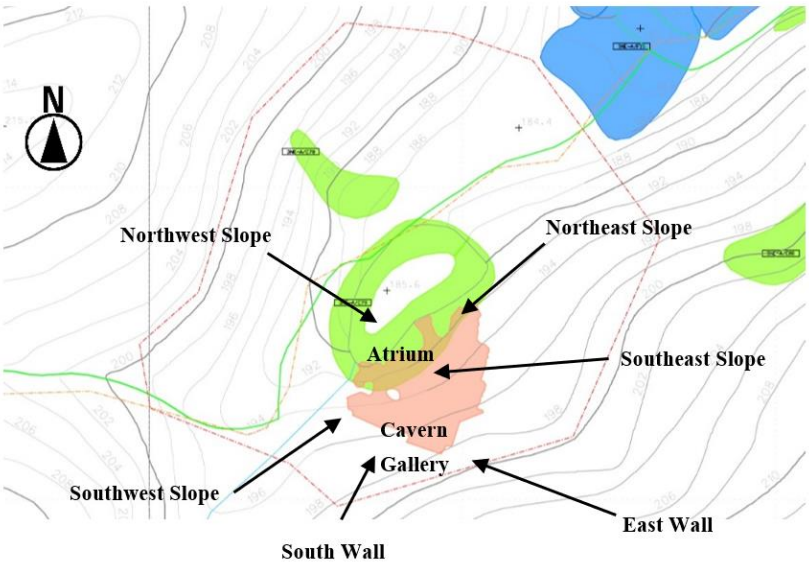

Figure 10: Location plan of slope faces and cavern walls

Table 6: Discontinuity data from manual and laser scan processing

Slope Face (Refer to Figure 10)	Joint Set	Manual Discontinuity Survey		Laser Scan derived Discontinuity Survey	
		Dip Angle	Dip Direction	Dip Angle	Dip Direction
Southeast	J1	43	102	47	129
	J2	45	043	46	039
	J3	85	312	79	295
	J4	25	116	88	172
	J5	48	142	87	098
Northwest	J1	30	100	37	119
	J2	63	116	62	121
	J3	48	052	35	067
	J4	52	144	90	309
Northeast	J1	70	062	60	045
	J2	50	200	63	223
	J3	76	180	74	191
Southwest	J1	72	092	/	/
	J2	51	113	/	/
	J3	70	338	/	/
	J4	85	270	/	/
	J5	75	120	/	/

For the southeast slope face (i.e., Rock cut slope at the atrium outside Cavern), both laser scan and manual survey identify similar major joint sets (J1, J2, and J3) with fairly consistent orientation. For the northwest slope face, both laser scan and manual survey identify similar major joint sets (J1, J2, and J3) with fairly consistent orientation. For the northeast slope face, both laser scan data and manual survey identify similar major joint sets (J1, J2, and J3) with fairly consistent orientation. For the southwest slope face, no laser scan discontinuity data is available due to dense vegetation. Manual discontinuity survey identifies four major joint sets. J1 represents the shear plane parallel to the slope face, while J2 and J3 are the dominant joint sets identified within the cavern gallery and in other slope faces.

A kinematic stability assessment of the rock cut slope was carried out based on the major joint sets identified by portable laser scan and manual discontinuity survey. Kinematic analysis was completed using Rocscience computer software DIPS (v.6.0), the results of which are graphically presented in equal area stereoplot (lower hemisphere) using methods discussed by Hoek and Bray. The lateral limits of planar and toppling failure were set at ±20^{o} and ±10^{o}, respectively.

5 Conclusions

Portable laser scanning supported by high resolution aerial LiDAR surveys, desk study, API and site inspection and mapping have provided complementary information to develop an accurate 3D model of part of the Lin Ma Hang Mine. The caverns are confirmed to be part of a complex inter-connected network of abandoned mine workings. The workings include sub-horizontal adits, inclined stopes, pillar and room workings, as well as vertical shafts and inclined ore passes. The caverns form a part of the Level 6 workings, the highest recorded level of workings. Within the former mining area as a whole, aerial LiDAR has also greatly helped identify anthropogenic features on the natural hillsides surrounding the caverns such as abandoned building platforms, in particular those related to suspected mine workings. Site observations confirmed the presence of ruins and several suspected openings into the mine. The caverns of Level 6 are accessed from the surface via adits and archway openings

Proceedings DOI: 10.21467/proceedings.133
ISBN: 978-81-957605-1-0

Series: AIJR Proceedings
ISSN: 2582-3922

excavated into a rock cut slope. A large "gallery" with span up to 19m and height of up to 6m is supported by several rock pillars.

Portable laser scanning enabled development of a detailed geo-referenced 3D model of the existing cavern, rock pillars and connected adits and openings augmented by a detailed aerial LiDAR derived DTM. It is anticipated that subsequent rock stress analysis of the cavern opening geometry and associated openings and adits will be greatly facilitated. Automated recognition of joint face facets from the 3D model enabled capture of discontinuity data from otherwise inaccessible faces such as the cavern roof (crown). The detailed 3D model will be used to tailor the design of necessary but sympathetically selected and installed local stabilisation measures. The model can also form the baseline for subsequent cavern monitoring as well as future educational interactive or display use.

6 Declarations

6.1 Acknowledgements

The 2020 LiDAR survey data has been used with the consent of the Geotechnical Engineering Office of the Civil Engineering and Development Department, of the Government of the Hong Kong SAR.

6.2 Publisher's Note

AIJR remains neutral with regard to jurisdictional claims in published maps and institutional affiliations.

References

Chu, J., & Chan, J. 2015. Hong Kong Mining History (1st ed., pp. 19-41). ProjecTerrae.

Davis, S. G., and Snelgrove, A. K. 1956. Geology of the Lin Ma Hang Lead Mine, New Territories, Hong Kong.

Davis, S. G. and Snelgrove, A. K. 1964. The Geology of the Lin Ma Hang Lead Mine, New Territories, Hong Kong, carried in Symposium on land use and mineral deposits in Hong Kong Southern China and South-East Asia: proceedings of Golden Jubilee Congress of University of Hong Kong. Hong Kong University Press

Dewez, T. J., Girardeau-Montaut, D., Allanic, C., and Rohmer, J. 2016. Facets: A Cloudcompare Plugin to Extract Geological Planes from Unstructured 3D Point Clouds. International Archives of the Photogrammetry, Remote Sensing & Spatial Information Sciences, 41.

GEO. 1991. Hong Kong Geological Survey (HKGS) Map Sheet 3, Solid and Superficial Geology, Sheung Shui, 1: 20,000 – scale, HGM20 series.

GEO. 1996. Hong Kong Geological Survey Memoir No.5 - Geology of the Northeastern New Territories. pp. 28,99-100,119,122 Government of Hong Kong.

GEO. 2018. Guide to Cavern Engineering. Geoguide 4. Geotechnical Engineering Office, Civil Engineering and Development Department, HKSAR Government, 262 p.

Grimstad, E. 1993. Updating the Q-system for NMT. In Proceedings of the International Symposium on Sprayed Concrete-Modern use of wet mix sprayed concrete for underground support, Fagemes, Oslo, Norwegian Concrete Association, 1993.

Idrees, M. O. and Pradhan, B. 2018. Geostructural Stability Assessment of Cave Using Rock Surface Discontinuity Extracted from Terrestrial Laser Scanning Point Cloud. Journal of Rock Mechanics and Geotechnical Engineering, 10(3), 534-544.

Kazhdan, M., Chuang, M., Rusinkiewicz, S. and Hoppe, H. 2020. Poisson Surface Reconstruction with Envelope Constraints. In Computer graphics forum (Vol. 39, No. 5, pp. 173-182).

Martin, C. D. and Maybee, W. G., 2000. The Strength of Hard Rock Pillars. Int. Jnl. Rock Mechanics & Min. Sci. 37:1239-1246.

Mellor, T. 2018a, April 27. Lin Ma Hang Mine Part 3 – Exploitation. The Industrial History of Hong Kong Group. https://Industrialhistoryhk.Org/Lin-Ma-Hang-Part-3-Exploitation/.

Mellor, T. 2018b, January 30. Lin Ma Hang Mine Part 2 – The Yung Years. The Industrial History of Hong Kong Group. https://industrialhistoryhk.org/lin-ma-hang-mine-part-2-the-yung-years/

Mellor, T. 2018c, May 30. Lin Ma Hang Mine Part 4 – Decline and Closure. The Industrial History of Hong Kong Group. https://industrialhistoryhk.org/lin-ma-hang-part-4-decline-and-closure/.

Mellor, T. 2021, January 9. Lin Ma Hang Mine Part 1 – The Early Years. The Industrial History of Hong Kong Group. https://industrialhistoryhk.org/lin-ma-hang-mine-part-1-the-early-years/

Norwegian Geotechnical Institute. 2015. Using the Q-system: Rock Mass Classification and Support Design.

Williams, T. 1991. The Story of Lin Ma Hang Lead Mine, 1915-1962. GSHK Newsletter, 9(4). pp. 3-26.

Wong, Jeffrey. 2021. Detector in the Air – 2020 Airborne LiDAR Survey. Joint Technical Symposium on Digital Geosciences & Geotechnology. 16 September 2021.

阮志 2012。《中港邊界的百年變遷：從沙頭角蓮蔴坑村說起》。香港：三聯書店（香港）有限公司。